Neurotherapeutics (2023) 20:325–337
https://doi.org/10.1007/s13311-022-01327-3

ORIGINAL ARTICLE

Gpr83 Tunes Nociceptor Function, Controlling Pain

Yerin Kim[1] · Chaeeun Kim[1] · Hojin Lee[1] · Minseok Kim[1] · Haiyan Zheng[1] · Ji Yeon Lim[1] · Hye-In Yun[1] · Minji Jeon[1] · Jungmin Choi[1] · Sun Wook Hwang[1]

Accepted: 27 October 2022 / Published online: 9 November 2022

Abstract

The function of peripheral nociceptors is frequently tuned by the action of G protein-coupled receptors (GPRs) that are expressed in them, which contribute to pain alteration. Expanding new information on such GPRs and predicting their potential outcomes can help to construct new analgesic strategies based on their modulations. In this context, we attempted to present a new GPR not yet acknowledged for its pain association. Gpr83 exhibits relatively high expressions in the peripheral nervous system compared to other tissues when we mined and reconstructed Gene Expression Omnibus (GEO) metadata, which we confirmed using immunohistochemistry on murine dorsal root ganglia (DRG). When Gpr83 expression was silenced in DRG, neuronal and behavioral nociception were all downregulated. Pathologic pain in hind paw inflammation and chemotherapy-induced peripheral neuropathy were also alleviated by this Gpr83 knockdown. Dependent on exposure time, the application of a known endogenous Gpr83 ligand PEN showed differential effects on nociceptor responses in vitro. Localized PEN administration mitigated pain in vivo, probably following Gq/11-involved GPR downregulation caused by the relatively constant exposure. Collectively, this study suggests that Gpr83 action contributes to the tuning of peripheral pain sensitivity and thus indicates that Gpr83 can be among the potential GPR targets for pain modulation.

Keywords Gpr83 · Pain · Analgesia · Nociceptor · PEN

Introduction

Confronted with a large unmet need for pain-reducing strategies, attempts to approach new therapeutic principles based on the excavation of novel targets are required, particularly from a component in the pain circuit that often experiences plastic changes [1, 2]. As the very front of those components, nociceptor neurons of dorsal root ganglia (DRG) play important roles in monitoring a noxious environment and generating and relaying pain signals [3]. Tuning the nociceptor sensitivity significantly affects the pain state, and the intrinsic molecular tuners expressed in those neurons may provide a new avenue for future analgesic translations because the active mimicking or intervention of their actions could be evolved to a useful proof of concept [2, 4, 5]. In this regard, G-protein coupled receptors (GPRs) comprise a well-known category of molecules for potentially serving such a tuning role. A number of GPRs such as opioid receptors and prostaglandin receptors have been shown for their contribution to altering pain states, and their modulators are clinically available for controlling pain [6, 7]. Nonetheless, patients frequently suffer from the low efficacies and/or serious adverse effects due to relatively low tissue specificity and/or growing resistance, of both the receptors and agents [1, 8].

Despite various other GPRs being expressed in the pain-associated neural circuit, the slow extension of their mechanistic information seems to limit constructing an alternative therapeutic strategy based on it. In this context, a better understanding of the identities of nociceptor-expressed but experimentally unexplored GPRs by assessing their pain outcomes may help to diversify their developmental opportunities. Gpr83 was initially cloned decades ago and was recently deorphanized [9–13]. According to the collective form of mammalian tissue expression profile generated from All RNA-seq and ChIP-seq sample and signature search (ARCHS[4]), an interface that mines and curates the whole of Gene Expression Omnibus (GEO) and Sequence Read Archive (SRA)

Yerin Kim and Chaeeun Kim contributed equally.

✉ Sun Wook Hwang
sunhwang@korea.ac.kr

[1] Department of Biomedical Sciences, Korea University College of Medicine, Seoul 02841, Korea

metadata stored in National Center for Biotechnology Information (NCBI), Gpr83, has the greatest expression in sensory neurons (Fig. S1) [14]. Therefore, we attempted to examine the role of Gpr83 in nociceptor-mediated pain. We hypothesized that Gpr83 endogenously tunes nociceptor functions, consequently regulating pain phenotypes. We also tested whether ligand-based external modulation of Gpr83 may aberrate the pain outcome.

Materials and Methods

Animals

Six-week-old male ICR mice were used in all experiments. Mice were kept at five per cage under 12-h light–dark cycle conditions. All animal work was performed under the national guidelines and the institutional animal care guidelines of the Institutional Animal Care and Use Committee of Korea University College of Medicine (2017–0146). Mice were acclimated to the test environment for 30 min before performing the following assays.

Nociceptive Behavioral Assays

Time engaged in hind paw licking and flicking behavior was quantitated for ~ 5 min as previously described [4, 15, 16]. To elicit Trpv1 activation-evoked behaviors, 100 ng capsaicin-containing 10 µl saline was intraplantarly injected,for eliciting Trpa1 activation-evoked behaviors, 26.4 µg cinnamaldehyde in 20 µl saline was injected.

For the complete Freund's adjuvant (CFA)-induced inflammation, 10 µl CFA was administered into a hind paw. For determining changes in mechanical or thermal behaviors by 24-h and/or 48-h CFA inflammation, Hargreaves assay (using Plantar Analgesia Meter; IITC, Woodland Hills, CA, USA) for acute heat avoidance or thermal hyperalgesia and von Frey assay by up-and-down paradigm (using von Frey filaments; Stoelting, Dale Wood, IL, USA) for mechanical allodynia were carried out as described previously [17, 18].

For the induction of neuropathic pain, the paclitaxel-induced chemotherapy-induced peripheral neuropathy (CIPN) model was used as described previously [19]. Briefly, paclitaxel was diluted in 1:1 ethanol and Cremophor EL and was intraplantarly injected at a dose of 4 mg/kg, once every 2 days. To check CIPN-induced cold allodynia, an acetone evaporation test was performed as described previously [20]. Briefly, 10 µl of acetone was taken first with a 200-µL micropipette and then was propelled via air burst on the hind paw of the mouse placed on the mesh under video recording for 60 s. The durations that animals were licking, shaking, and/or lifting were analyzed using slow-motion replay mode.

Cell Cultures

All cells were grown at 37 °C and 5% CO_2 and were used at 48–72 h after culture. Primary cultures of DRG neurons were prepared as described previously [21]. Briefly, DRG was isolated from mice and was treated with 1.5 mg/ml of collagenase A/dispase II at 37 °C for 45 min and then treated with 0.25% trypsin for a further 7 min. Subsequently, the cell pellets were suspended with DNase. Dispersed neurons were plated onto poly-L-lysine-coated glass cover slips in Dulbecco's Modified Eagle Medium F-12 containing 10% fetal bovine serum and 1% penicillin/streptomycin. Experiments using neuronal cultures were performed 24–72 h after plating.

Fluorescence Intracellular Ca^{2+} Imaging Experiments

Ca^{2+} imaging experiments were carried out as described previously [22]. Briefly, cells were loaded with 5 µM Fura-2AM dye and 0.02% pluronic F127 for 30 min. The cells were resuspended in 140 mM NaCl, 5 mM KCl, 2 mM $CaCl_2$, 1 mM $MgCl_2$, 10 mM D-glucose, and 10 mM HEPES (titrated to pH 7.4 with NaOH). Images of dye-loaded cells were obtained with a cooled CCD camera (Retiga-SRV, Q-imaging Corp., Burnaby, BC, Canada). The ratio of fluorescence intensity at 340 nm/380 nm wavelengths in each experiment was analyzed using MetaFluor (Molecular Devices, Sunnyvale, CA, USA). Following agonist treatment, when the fluorescence increased by 1% or more compared to the baseline, we determined that an agonist-induced response had occurred.

Luciferase Assays

We followed the manufacturer's protocol provided for the ONE-Glo™ EX Luciferase Assay System (E8110; Promega, Madison, WI, USA). Briefly, the Lipofectamine-vector complex was added to cells seeded in a 96-well plate. Three luciferase reporter vectors were used: pGL4.29[luc2P/CRE/Hygro], pGL4.30[luc2P/NFAT-RE/Hygro], and pGL4.33[luc2P/SRE/Hygro] (Promega). At the same time, the murine Gpr83 (mGpr83) plasmid DNA pRP[Exp]-EGFP/Puro-CAG > mGpr83[NM_010287.3] (VectorBuilder Inc, Chicago, IL, USA) was also transfected in serum reduced media. After 24 h, the luciferase reagent was added to induce the expression of the luciferase gene, and the luminescence was measured by Gen5™ Version 2.0 Data Analysis Software (Bio-Tek Instruments Inc., Winooski, VT, USA).

Transfections

The murine Gpr83 small interfering RNA (siRNA) and scramble RNA (scRNA) were designed and synthesized by Bioneer Corporation (Daejeon, Korea). Target sequences for siRNA were sense-UGACCUUGGCUCUAUCCAU and antisense-AUGGAUAGAGCCAAGGUCA). For the transfection of siRNA or scRNA in vivo, 3 μg of RNA and 5% D-glucose in 7 μg of Lipofectamine 2000 were injected into the spinal cord daily from 96 h before experiments or near the ipsilateral sciatic nerve one time 24 h before experiments. The HEK293 cell transfections in vitro were carried out with the use of Lipofectamine 2000 reagent on DRG neurons following the manufacturer's instructions. Lipofectamine 2000 (1 μl) was added to 50 μl of Opti-MEM and incubated at room temperature for 5 min. Then, 20 pmol of siRNA or scRNA were added and further incubated at room temperature for 20 min. For the mGpr83 plasmid, 20 μg was used instead. The lipofectamine-including complexes were added to culture plate (50 μl per well), and the media were replaced with fresh ones after 4–6 h. After a further 24–96 h, the experiment was performed.

Immunohistochemistry

Immunohistochemical analysis was conducted as described previously [4]. Briefly, lumbar DRG were prepared from mice. Fourteen-micrometer sections were prepared using a Leica CM3050s cryotome (Leica Microsystems, Wetzlar, Germany) and permeabilized with 0.2% Triton-X100 for 1 h. Together with a pan nuclear marker 4′,6-diamidino-2-phenylindole (DAPI) treatment, samples were then stained with anti-Gpr83 (rabbit, 1:100; LSbio. Seattle, WA, USA), anti-Trpv1 (mouse, 1:100; Abcam, Cambridge, UK), anti-trpm8 (goat, 1:300, Antibodies-online, Aachen, Germany), anti-substance P (mouse, 1:500, Abcam), and/or anti-calcitonin gene-related peptide (CGRP) (goat, 1:2000; Abcam) antibodies. After 24 h at 4 °C, sections were stained with secondary antibodies (Alexa 594-labeled or Alexa 488-labeled secondary antibodies; Thermo Fisher, Rockford, IL, USA) for 1 h at room temperature and placed under a coverslip, followed by image acquisition with the iRiS Digital imaging system (Logos Biosystems, Anyang, Korea) and/or Zeiss LSM 800 confocal microscope (Carl Zeiss, Oberkochen, Germany).

Western Blot Analysis

Cells were homogenized in radioimmunoprecipitation assay (RIPA) cell lysis buffer (Elpisbio, Daejeon, Korea) containing protease inhibitors and phosphatase inhibitors using a tissue homogenizer. The total homogenized suspension was centrifuged at 15,000 × *g* for 15 min and then separated by sodium dodecyl sulfate–polyacrylamide gel electrophoresis (SDS-PAGE) for western blotting (Bio-Rad, Hercules, CA, USA). The transferred polyvinylidene fluoride (PVDF) membranes were then blocked with 5% bovine serum albumin (BSA) solution for 1 h, at room temperature. The membranes were probed with anti-Phospho-p44/42 mitogen-activated protein kinase (ERK1/2) (1:2000, #4270 s; Cell Signaling Technology, Danvers, MA, USA) or ERK1/2 (1;2000, #4696 s; Cell Signaling Technology) or mouse monoclonal anti-β-actin (ab8226, 1:10,000, Abcam) antibodies at 4 °C. After 24 h, the membranes were incubated with horseradish peroxidase-conjugated goat anti-mouse antibodies (G21040, 1:2000, Invitrogen, Carlsbad, CA, USA) or horseradish peroxidase-conjugated goat anti-rabbit antibodies (G21234, 1:2000, Invitrogen) and were visualized by the addition of the ECL Western Blotting Substrate (Thermo Fisher). The resultant immunofluorescence was quantified using ImageJ software (National Institutes of Health, USA).

Subclustering Analysis of RNA-Sequencing Data

Single-cell RNA-sequencing (scRNA-seq) and single nucleus RNA-sequencing (snRNA-seq) datasets from Gene Expression Omnibus (GEO) accession numbers GSE139088 and GSE154659, respectively, were used as raw data. Gene count matrix log-normalization (10,000 scale factor), gene clustering, dimension reduction analysis (universal manifold approximation and projection; UMAP), differential gene expression analysis, and plotting were conducted using R (version 4.1.2) and Seurat (version 4.0.6). The data was imputed for denoising with Markov affinity-based graph imputation of cells (MAGIC, $t = 8$).

Compounds

All chemicals were purchased from Sigma-Aldrich (St. Louis, MO, USA) unless otherwise described. Paclitaxel, mouse PEN (mPEN), and human PEN (hPEN) were purchased from Tocris Bioscience (Ellisville, MO, USA). Cinnamaldehyde was purchased from MP Biomedicals (Solon, OH, USA). Cremophor EL was purchased from Merck KGaA (Darmstadt, Germany). Dispase II was purchased from Roche Diagnostics (Indianapolis, IN, USA). Trypsin and Lipofectamine 2000 were purchased from Invitrogen. Dulbecco's Modified Eagle Medium F-12 and Opti-MEM were purchased from Thermo Fisher. Fetal bovine serum was purchased from HyClone Laboratories (Logan, UT, USA). Phosphatase inhibitors were purchased from Roche Diagnostics. Stock solutions were prepared using water or dimethyl sulfoxide and diluted with test solutions before use.

Data Analysis

Statistical significance of data was assessed using the two-tailed unpaired Student's t-test, one-way analysis of variance (ANOVA) followed by Bonferroni's post hoc test, or two-way ANOVA followed by Tukey's post hoc test (*** $p < 0.001$, ** $p < 0.01$, * $p < 0.05$). Data are shown as the means ± S.E.M.

Results

Gpr83 Is Expressed in DRG Neurons

When we reconstructed ARCHS^4-based GEO data calculations, Gpr83 expression in the peripheral sensory neuron class was at the highest levels throughout the tissues (Fig. S1). We investigated whether this expression of Gpr83 is reproducible in somatosensory neurons in separate datasets by analyzing massive RNA-seq data (GSE139088 and GSE154659) from two recent independent studies on murine DRG neurons [23, 24]. UMAP-based construction of their raw transcriptomic resources identified a subset of Gpr83 expresser cells in approximately a dozen clusters (Fig. 1A–B). Our immunohistochemistry confirmed DRG neuronal expression of Gpr83, which is selectively reduced by RNA interference (RNAi) (Figs. S2 and 1C). We considered whether pain-mediating nociceptor neurons express Gpr83 and profiled co-expressions with four other nociceptive genes including Tac1 (encoding substance P), Calca (encoding calcitonin gene-related peptide), Trpm8 (transient receptor potential melastatin subtype 8), and Trpv1 (transient receptor potential vanilloid subtype 1) using the reconstructed UMAP representations of GSE139088 (Fig. 1D–G) and GSE154659 datasets (Fig. 1L–O). Consequently, we found that the Gpr83-positive subclusters from the two independent RNA-seq datasets commonly express the four pain-related genes to an extent, and almost all Gpr83-expresser neurons also express the gene encoding substance P, a crucial neuropeptide for mediating pathologic pain (Fig. 1H–K and P–S). The result indicates that Gpr83 may

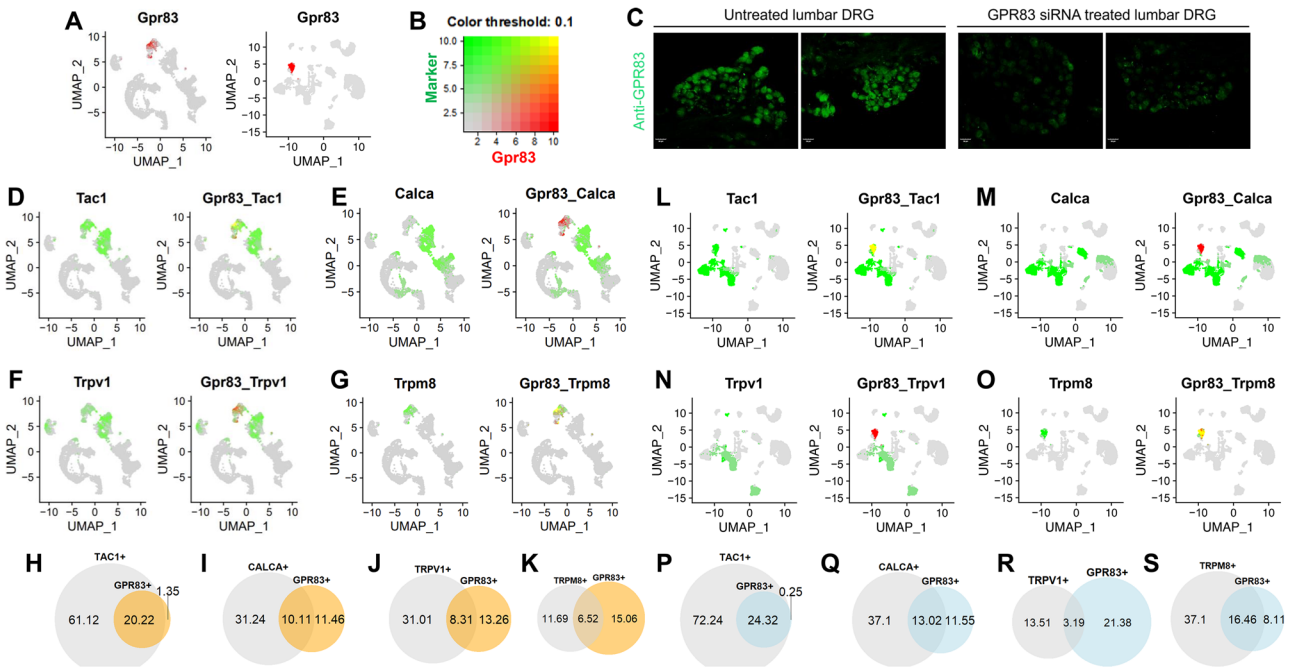

Fig. 1 Gpr83 expression in a subset of DRG neurons. **A** Universal manifold approximation and projection (UMAP) representation of graph-based clustered single-cell RNA sequences (GSE139088, left) and single nucleus RNA sequences (GSE154659, right) from mouse dorsal root ganglionic cells revealed Gpr83-expressing subclusters (red). **B** Two-dimensional color codes used for simultaneously visualizing the co-expressions of Gpr83 (red) and marker (green) RNAs in plots from *(D)* to *(G)* and from *(L)* to *(O)*. **C** Two representative immunohistochemical images of Gpr83 expression (green) in mouse DRG sections with (right two images) or without Gpr83 small interfering RNA (siRNA) treatment (left two images). **D–G** UMAP representations for visualizing Gpr83 and marker expression in the GSE139088 dataset. Tac1 *(D)*, Calca *(E)*, Trpv1 *(F)*, and Trpm8 *(G)* were used as markers. **H–K** Venn diagrams of which the relative sizes reflect the numbers of Gpr83 expresser cells and their co-expression profiles with the four markers presented in *(D)* to *(G)*. **L–O** UMAP representations for visualizing Gpr83 and marker expression in the GSE154659 dataset. Tac1 *(L)*, Calca *(M)*, Trpv1 *(N)*, and Trpm8 *(O)* were used as markers. **P–S** Venn diagrams of which the relative sizes reflect the numbers of expresser cells of Gpr83 and their co-expression profiles with the four markers presented in *(L)* to *(O)*.

be involved in nociceptor functions and possibly associated with pain sensation.

Gpr83 Tunes Nociceptor Functions

We then hypothesized that Gpr83 may modulate nociceptor functions and thus examined the effect of RNAi-induced Gpr83 silencing in cultured DRG neurons (Fig. 1D). When we applied capsaicin, a Trpv1-specific agonist to those neurons in fluorescent intracellular Ca^{2+} imaging, significant reduction both in the number of capsaicin responder neurons and in their peak responses were observed in the neurons with Gpr83 knockdown, compared to wild type neurons or neurons treated with a scrambled RNA (scRNA) (Fig. 2A, B). Applications of cinnamaldehyde, an agonist for another nociceptive ion channel transient receptor potential ankyrin subtype 1 (Trpa1), showed a similar tendency in the reductions (Fig. 2C, D). The results suggest that the presence or absence of Gpr83 may readily affect nociceptor functions in vitro. We then considered whether these results in vitro could be reproduced in TRP-specific peripheral modality assays in vivo. Mice with Gpr83 knockdown were generated using peri-sciatic and intrathecal siRNA treatment and then were acutely exposed to capsaicin and cinnamaldehyde using an intraplantarly injection to the hind paws. As a result, the acute nociceptive behaviors for which Trpv1 and Trpa1 are specifically responsible were both significantly reduced (Fig. 2E, N). Therefore, with consistency, both in vivo and in vitro results commonly suggest that the presence of Gpr83 in nociceptors may tune the functionality of nociceptors and that it probably leads to a positive orientation for promoting pain sensation.

Gpr83 Affects Pathologic Pain

We then hypothesized that Gpr83 in nociceptors may also tune nociception under pathologic states in vivo. We first examined the Gpr83 knockdown effect in CFA-induced inflammatory pain in hind paws. Compared to animals treated with scRNA, the siRNA-treated groups showed statistically milder phenotypes in both mechanical allodynia and thermal hyperalgesia (Fig. 3A–D). We further tried to test this hypothesis on a clinically relevant pathologic pain model and used paclitaxel-induced CIPN model. Its typical pain phenotypes such as mechanical and cold allodynia were also milder when Gpr83 was pre-emptively knocked down (Fig. 4A–E). We further considered whether the contribution of Gpr83 is maintained in the middle of developing CIPN-induced pain, and the knockdown effect can occur during the pain period. Accordingly, we administered siRNA on day 3, the time when the pain first reaches the plateau period. Although there was a slight delay, both mechanical and cold allodynia was significantly reduced compared to those from the scRNA-treated group, indicating that Gpr83 constantly contributes to the pain state (Fig. 4F–J). Collectively, the results suggest that Gpr83 may contribute to the tuning of nociception under pathologic states and thus possibly be a target molecule to control such pain.

PEN Alters Nociceptor Function and Pain

PEN, an endogenous peptide product derived from the multiple enzymatic cleavages of the proSAAS protein, has been shown to specifically activate Gpr83. Therefore, we asked whether PEN could modify DRG neuronal function. Whereas voltage-gated channel mediated responses monitored by KCl depolarization-induced increases in intracellular Ca^{2+} were tolerant to the absence or presence of PEN, capsaicin-induced and Trpv1-mediated increases in intracellular Ca^{2+} were altered by PEN exposure (Fig. 5). Interestingly, dependent on how we set the response cutoff and how long the PEN exposure time was, differential PEN effects were observed. When an increase of at least 1% from the baseline was set as a fluorescence response cutoff as in Fig. 2, exposure time-dependent decreases were observed in both the number of responder neurons and average fluorescence peaks when PEN was added, which indicates that PEN exposure may downregulate nociceptor functions (Fig. 5A–D). On the other hand, when a 10% increase from the baseline was set as a fluorescence response cutoff, 5-min PEN treatment promoted moderate Ca^{2+} fluorescence responses, whereas relatively long-term incubations with PEN tended to similarly diminish neuronal responses as in the case of setting a 1% increase (Fig. 5E–H). These results may indicate that a group of neurons, particularly with greater responsiveness may experience a transient enhancement in after responses by PEN exposure.

We considered whether such effects can be repeated in models in vivo, and we attempted to look at acute and inflammatory pain. Peripheral PEN treatment did not elicit any spontaneous behavior although it transiently reduced mechanical and thermal thresholds (Fig. 6A, B). On the other hand, spontaneous nociceptive behaviors in response to peripheral capsaicin treatment were moderately but significantly blunted by PEN (Fig. 6C, D). Furthermore, PEN treatment elevated both mechanical and thermal thresholds, which had been decreased under CFA-induced inflammation (Fig. 6E–H). Therefore, the data indicate that PEN treatment, particularly in the longer term may have a pain-reducing potential.

GPRs can often experience multiple downstream signals and activation-dependent downregulation as well, which has already been suggested for Gpr83-mediated mechanisms [25, 26]. We tried to briefly repeat whether such intracellular changes may be related to PEN-induced complicated outcomes. As reported previously, both Gq/11 and

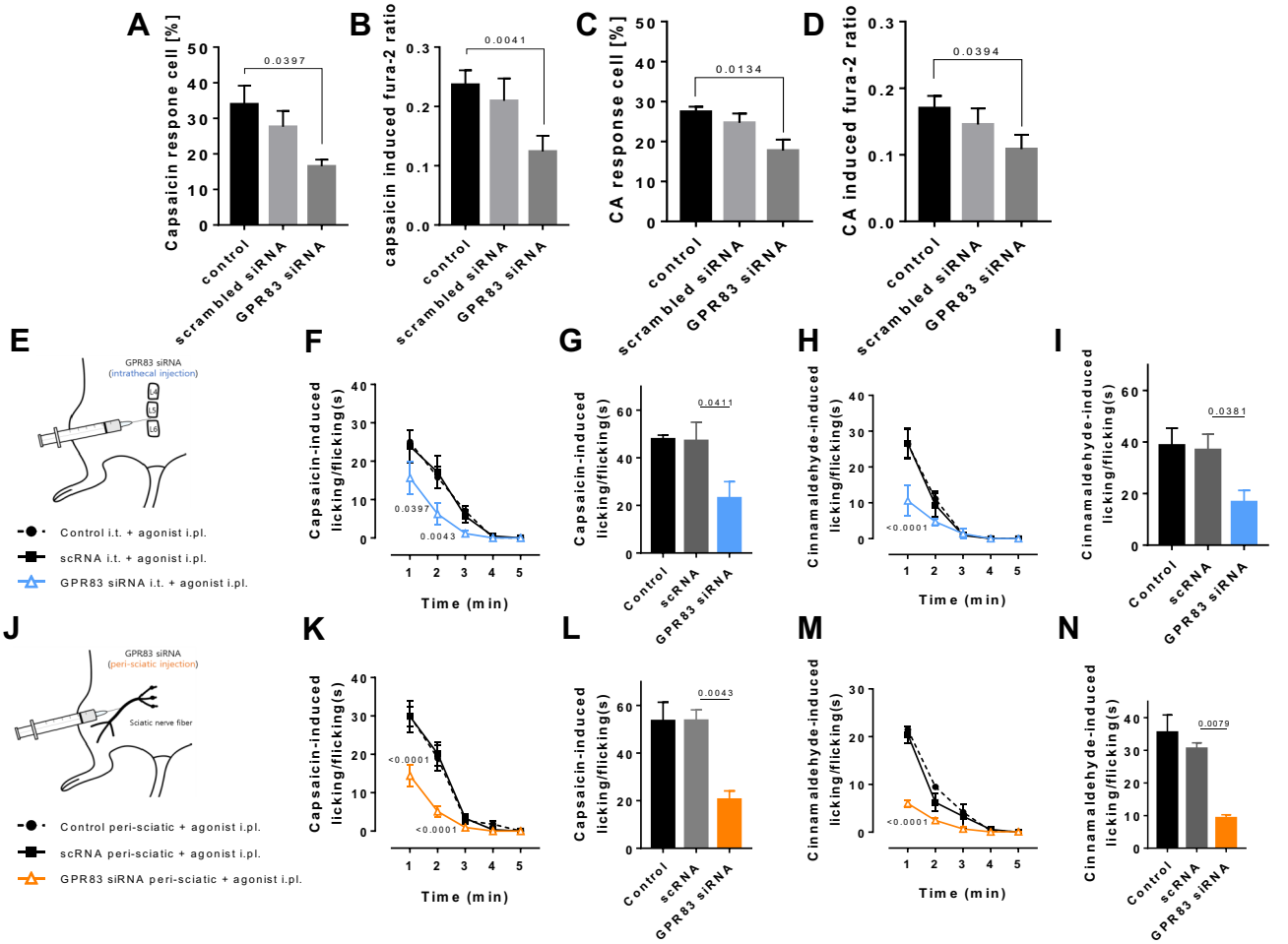

Fig. 2 Gpr83 knockdown alters nociceptor functionalities. **A** Percentage of capsaicin-responsive neurons with or without Gpr83 siRNA treatment or with scrambled RNA (scRNA) treatment in fura-2 intracellular Ca^{2+} imaging (control group, $n=4$ batches; siRNA-treated group, $n=3$ batches; scRNA-treated group, $n=3$ batches). **B** Peak increases in fluorescent levels of capsaicin-responsive neurons in (***A***), with or without Gpr83 siRNA treatment or with scRNA treatment in fura-2 intracellular Ca^{2+} imaging (control group, $n=317$ neurons; siRNA-treated group, $n=158$ neurons; scRNA-treated group, $n=109$ neurons). Experiments in (***A–B***) were triplicated. **C** Percentage of cinnamaldehyde-responsive neurons with or without Gpr83 siRNA treatment or with scRNA treatment in fura-2 intracellular Ca^{2+} imaging (control group, $n=5$ batches; siRNA-treated group, $n=4$ batches; scRNA-treated group, $n=5$ batches). **D** Peak increases in fluorescent levels of cinnamaldehyde-responsive neurons in (***C***) with or without Gpr83 siRNA treatment or with scRNA treatment in fura-2 intracellular Ca^{2+} imaging (control group, $n=320$ neurons; siRNA-treated group, $n=164$ neurons; scRNA-treated group, $n=168$ neurons). Experiments in (***C–D***) were triplicated. **E** A schematic diagram for interfering Gpr83 expression in DRG using a peri-sciatic injection of siRNA. Five animals were used for each experiment. **F** Time course of the duration of 0.1% capsaicin (CAP)-induced nociceptive behaviors in mice with or without peri-sciatic injection of Gpr83 siRNA and with that of scRNA. CAP was administered intraplantarly in a hind paw. **G** Total durations of nociceptive responses for 5 min from (***F***) are quantified in the histogram. **H** Time course of the duration of 10 mM cinnamaldehyde (CA)-induced nociceptive behaviors in mice with or without peri-sciatic injection of Gpr83 siRNA and with that of scRNA. CA was injected intraplantarly into a hind paw. **I** Total durations of nociceptive responses for 5 min from (***H***) are quantified in the histogram. **J** A schematic diagram for interfering Gpr83 expression in DRG using an intrathecal injection of siRNA. Five animals were used for each experiment. **K** Time course of the duration of 0.1% CAP-induced nociceptive behaviors in mice with or without peri-sciatic injection of Gpr83 siRNA and with that of scRNA. CAP was intraplantarly injected into a hind paw. **L** Total durations of nociceptive responses for 5 min from (***K***) are quantified in the histogram. **M** Time course of the duration of 10 mM CA-induced nociceptive behaviors in mice with or without peri-sciatic injection of Gpr83 siRNA and with that of scRNA. CA was intraplantarly injected into a hind paw. **N** Total durations of nociceptive responses for 5 min from (***M***) are quantified in the histogram. Intracellular fluorescent Ca^{2+} responses in *(A)–(D)* were compared with those without RNA injection by one-way ANOVA and Tukey's test. Effects on the durations of the nociceptive responses in *(E)–(N)* at every minute were compared with those without RNA injection by two-way ANOVA and Tukey's test, and the comparisons between total durations were conducted by one-way ANOVA and Tukey's test

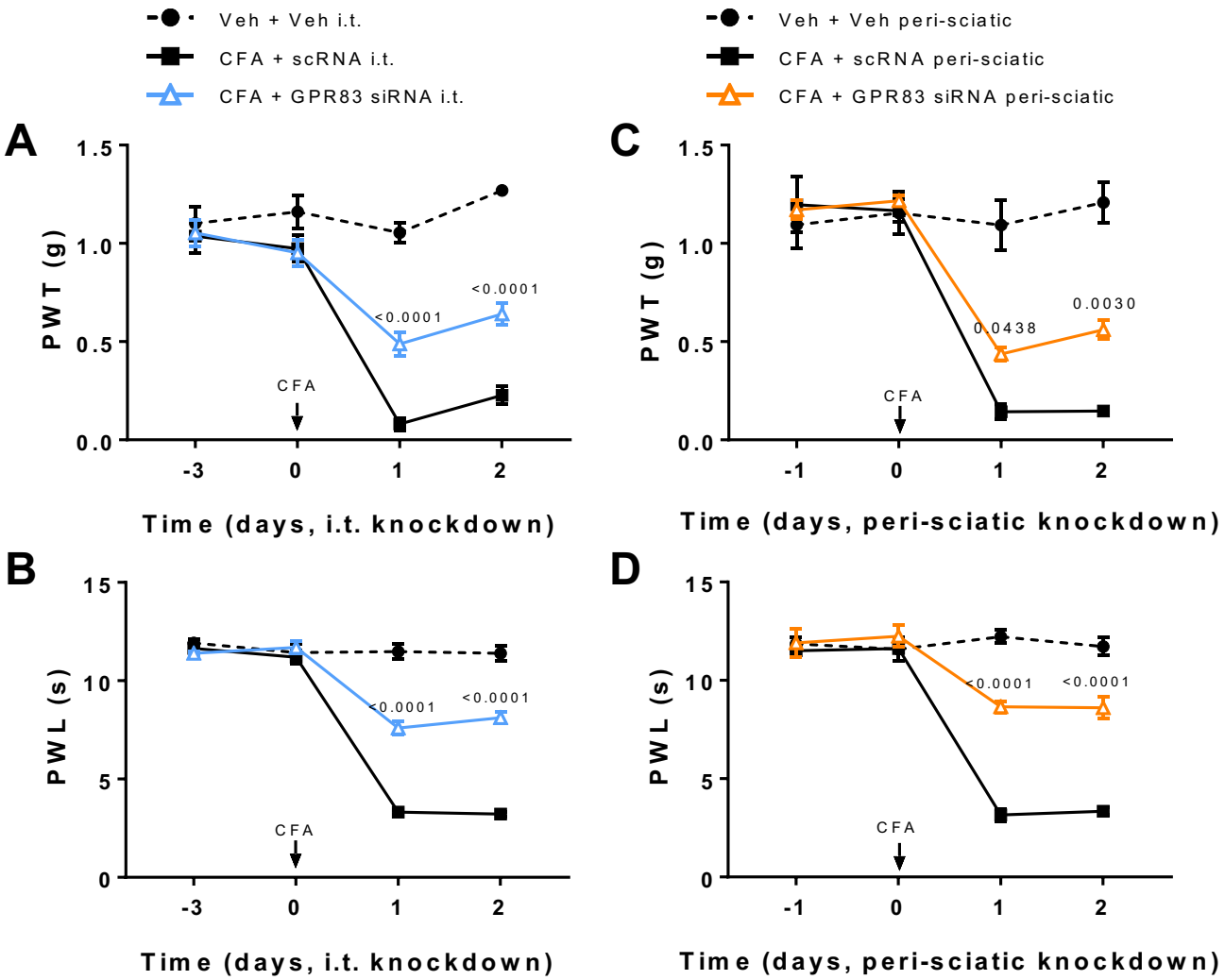

Fig. 3 Gpr83 knockdown alleviates inflammatory pain. **A** Time course of von Frey thresholds in complete Freund's adjuvant (CFA)-inflamed mice. Animals were intrathecally pretreated with siRNA or scRNA, and their thresholds were monitored 24 h and 48 h after CFA injection. The dots in the plot show individual threshold values. **B** Time course of Hargreaves latencies in CFA-inflamed mice. Animals were treated in the same manner as in *(A)*. The dots in the plot show individual latency values. **C** Time course of von Frey thresholds in CFA-inflamed mice. Animals were administered peri-sciatically with siRNA or scRNA, and their thresholds were monitored 24 h and 48 h after CFA injection. The dots in the plot show individual threshold values. **D** Time course of Hargreaves latencies in CFA-inflamed mice. Animals were treated in the same manner as in *(C)*. The dots in the plot show individual latency values

Gi/o-mediated signaling seems to be affected by PEN incubation in our Gpr83-overexpressing cell line-based signaling assays (Fig. 7). Increases in the serum response element (SRE)-mediated luminescence even without PEN indicated Gpr83-mediated constitutive Gq/11 activation and subsequent protein kinase C (PKC)-mediated extracellular signal-regulated kinase (ERK) signaling (Fig. 7A), which may explain its in vivo and in vitro knockdown results above. The presence of PEN caused the luminescence to decrease, indicating the downregulation of that Gq/11-PKC-ERK axis, which may associate with PEN-induced pain reduction. On the other hand, the luminescence for the nuclear factor of activated T-cells response element (NFAT-RE), representing inositol triphosphate (IP_3)-mediated internal Ca^{2+} modification, another branch of Gq/11-dependent signals, seemed to less preferentially be affected (Fig. 7B). Decreases in the cAMP response element (CRE) suggest that Gi/o-mediated signaling is also coupled to Gpr83 and may contribute to PEN-induced pain reduction (Fig. 7C). Because these luminescence assays were rather optimized relatively for long-term ligand exposure, we examined the phosphorylation of ERK, a further downstream point for Gq/11- and β-arrestin-mediated Gpr83 signaling which enabled observations in a shorter time frame [27]. As a result, the phosphorylation was significantly increased under 5-min exposure of PEN, suggesting that PEN may first acutely activate and then

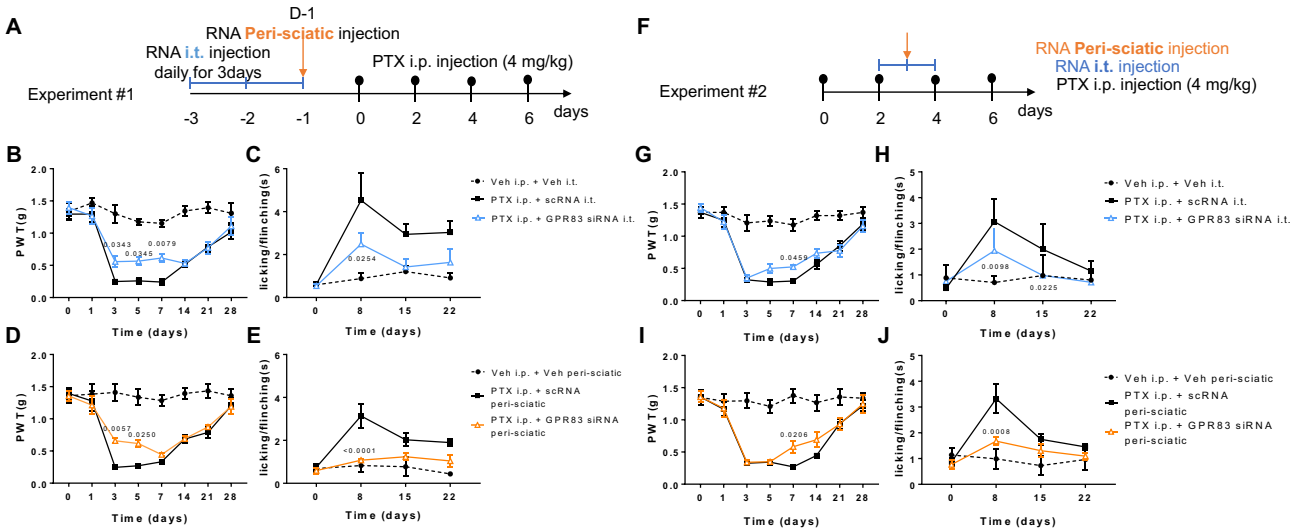

Fig. 4 Gpr83 knockdown alleviates chemotherapy-induced neuropathic pain. **A** Summary of the experimental schedule for (***B***) to (***E***). Pre-emptive siRNA or scRNA injection was followed by paclitaxel injections (intraperitoneal administration, 4 mg/kg). **B** Time course of von Frey thresholds in mice treated intrathecally as in (***A***) ($n=4$–5). **C** Time course of cold sensitivities in mice treated intrathecally as in (***A***) ($n=4$–5). **D** Time course of von Frey thresholds in mice treated peri-sciatically as in (*A*) ($n=4$–5). **E** Time course of cold sensitivities in mice treated peri-sciatically as in (***A***) ($n=4$–5). **F** Summary of the experimental schedule for (***G***) to (***J***). siRNA or scRNA was injected in animals during the paclitaxel treatment regimen as shown in (*A*). **G** Time course of von Frey thresholds in mice treated intrathecally as in (***A***) ($n=5$). **H** Time course of cold sensitivities in mice treated intrathecally as in (***A***) ($n=5$). **I** Time course of von Frey thresholds in mice treated peri-sciatically as in (***A***) ($n=5$). **J** Time course of cold sensitivities in mice treated peri-sciatically as in (***A***) ($n=5$)

downregulate Gpr83, as observed in Fig. 5E–H. Hence, although PEN exposure may transiently prompt pain via that acute Gq/11-mediated ERK effect, it may dampen pain on the longer-term basis via Gq/11 downregulation and Gi/o-coupled signaling. Collectively, Gpr83 appears to retain multi-potentials to elicit intracellular signalings including constitutive activation, Gq/11- and Gi/o-mediated mechanisms, and time-dependent ligand actions. Therefore, analgesic outcomes may occur not only by Gpr83 knockdown but also through treatment with PEN.

Overall, our results suggest that Gpr83 contributes to the tuning of DRG nociceptor functionality, thereby modulating pain states.

Discussion

Our study proposes a new GPR-coupled regulatory concept of pain. Peripheral nociceptor functions were significantly affected by Gpr83 knockdown, which was reproduced in phenotypic observations in vivo in normal and pathological states. Such data suggest that this GPR may constantly be contributing to the sensory neuronal and thus pain tone. The interpretation of outcomes from ligand applications seems to be more complex than those from other traditionally known ligands for pain-producing Gq/11- and Gs-coupled GPRs, including bradykinin and prostaglandins, the substances that give a relatively clear warning signal [6, 28]. It is possible that the physiological roles of Gpr83 may be more optimized for constitutive tuning than for surveilling a new environmental input. Despite being predicted as a tuner for neuronal function, it is interesting that it does not seem to affect voltage-gated components, namely the decision machinery responsible for generating electrical output. Based on our findings that sensory receptors and their modalities were primarily under Gpr83 influence instead, we can speculate that fine-tuning from signaling upstreams may selectively apply to differential nociceptive molecules and signaling layers. Therefore, a search for other possible selective targets of which the activities are under Gpr83 control may be of future interest as well. Upstream signals also have the potential to diversify into many forms, for example, receptor isotypes, and they accordingly may affect a target in different ways. This study was open to collective outcomes from the downregulation of Gpr83 isoforms by designing siRNAs for influencing all reported splice variants of Gpr83. Differential signaling, if any, depending on isotypes from alternative splicing may need to be scrutinized in the future.

Our study offers the first evidence for functional modulation of peripheral neurons by Gpr83. Its hypothesis originated from neuronal expressions confirmed by our transcriptomic and histological analyses. The expression and function of Gpr83 have earlier been studied in other tissues as well. It is expressed in regulatory T cells and possibly contributes to immune tolerance [29]. Hypothalamic Gpr83 appears to play a role in feeding behaviors [30]. Other brain regions such

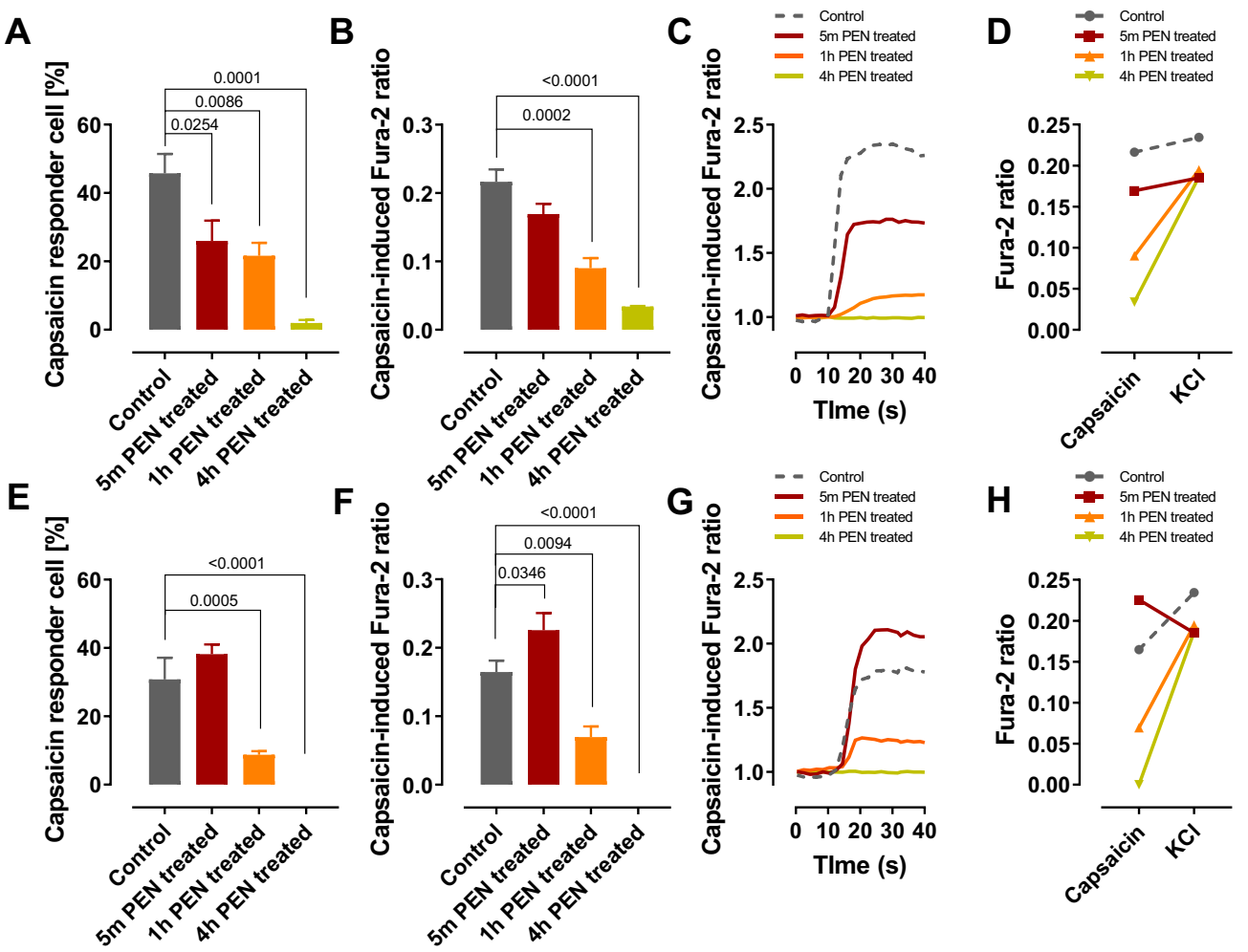

Fig. 5 Incubation time-dependent differential alteration of nociceptor functions by PEN. **A** Percentage of capsaicin-responsive neurons under PEN exposures in fura-2 intracellular Ca^{2+} imaging (untreated group, $n=4$ batches; 5-min PEN-treated group, $n=6$ batches; 1-h PEN-treated group, $n=8$ batches; 4-h PEN-treated group, $n=4$ batches). **B** Peak increases in fluorescent levels of capsaicin-responsive neurons in (***A***), with or without PEN treatment in fura-2 intracellular Ca^{2+} imaging (untreated group, $n=453$ neurons; 5-min PEN-treated group, $n=455$ neurons; 1-h PEN-treated group, $n=508$ neurons; 4-h PEN-treated group, $n=172$ neurons). Experiments in (***A–B***) were triplicated. **C** Representative traces of fura-2 intracellular Ca^{2+} levels from individual neurons. **D** Averaged fura-2 intracellular Ca^{2+} levels upon capsaicin and KCl-induced depolarization (untreated group, $n=453$ neurons; 5-min PEN-treated group, $n=455$ neurons; 1-h PEN-treated group, $n=508$ neurons; 4-h PEN-treated group, $n=172$ neurons). **E** Percentage of capsaicin-responsive neurons under PEN exposures in fura-2 intracellular Ca^{2+} imaging. When fluorescence increased in response to agonist treatment by 10% or more compared to the baseline before drug treatment using the same raw data with those in (***A***), we determined that an agonist-induced response had occurred (untreated group, $n=4$ batches; 5-min PEN-treated group, $n=6$ batches; 1-h PEN-treated group, $n=8$ batches; 4-h PEN-treated group, $n=4$ batches). **B** Peak increases in fluorescent levels of capsaicin-responsive neurons in (***E***), with or without PEN treatment in fura-2 intracellular Ca^{2+} imaging (untreated group, $n=451$ neurons; 5-min PEN-treated group, $n=198$ neurons; 1-h PEN-treated group, $n=108$ neurons; 4-h PEN-treated group, $n=171$ neurons). Experiments in (***A–B***) were triplicated. **C** Representative traces of fura-2 intracellular Ca^{2+} levels from individual neurons. **D** Averaged fura-2 intracellular Ca^{2+} levels upon capsaicin and KCl-induced depolarization (untreated group, $n=453$ neurons; 5-min PEN-treated group, $n=198$ neurons; 1-h PEN-treated group, $n=108$ neurons; 4-h PEN-treated group, $n=171$ neurons)

as the nucleus accumbens, striatum, and olfactory tubercle also seem to express Gpr83, but its cellular or neural impacts remain elusive [31]. In those fields, downstream signal transduction has currently been under investigation, and previous studies have proposed relatively repeatable principles using neuronal and adenocarcinoma cell lines and mammalian heterologous expression systems,Gq/11-mediated signaling activity was detected as a major constitutive pathway [32]. Later, activation by a ligand has been shown to lead not only to Gq/11-mediated signaling but also Gi/o- and β-arrestin-mediated cascades, and in addition, to ERK-dependent further downstream process [10, 27], which were reproduced

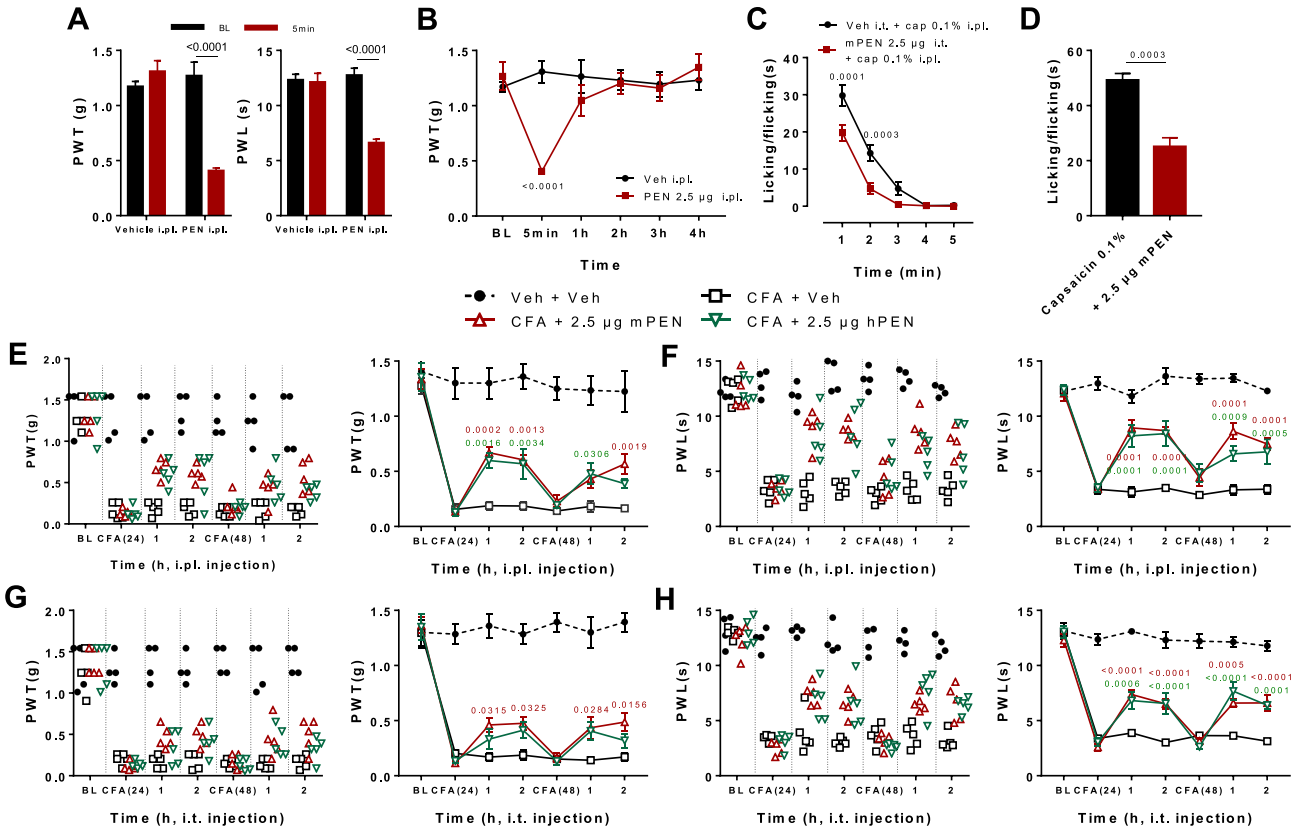

Fig. 6 PEN treatment alleviates pain. **A** von Frey thresholds (left) and Hargreaves latencies (right) immediately after intraplantarly injection of PEN (2.5 μg/10 μl) in a hind paw. **B** Time course of von Frey thresholds after intraplantarly injection of PEN (2.5 μg/10 μl) in a hind paw for 150 min. **C** Time course of the duration of 0.1% capsaicin (CAP)-induced nociceptive behaviors in mice immediately after intraplantarly injection of 2.5 μg/10 μl in a hind paw. CAP was administered intraplantarly in the ipsilateral hind paw. **D** Total durations of nociceptive responses for 5 min from (***C***) are quantified in the histogram. **E** Time course of von Frey thresholds in complete Freund's adjuvant (CFA)-inflamed mice. Animals were treated intraplantarly with PEN (2.5 μg/10 μl) in the ipsilateral hind paw. The left dot plot shows individual threshold values. **F** Time course of Hargreaves latencies in CFA-inflamed mice. Animals were treated in the same manner as in *(E)*. The left dot plot shows individual latency values. **G** Time course of von Frey thresholds in CFA-inflamed mice. Animals were treated intrathecally with PEN (2.5 μg/10 μl). The left dot plot shows individual threshold values. **H** Time course of Hargreaves latencies in CFA-inflamed mice. Animals were treated in the same manner as in *(G)*. The left dot plot shows individual latency values

here. Therefore, a more or less complex form of signal transduction appears to occur when Gpr83 is activated. Together with possible isoform-preferential downstream signals as mentioned above, matrix-like approaches may be required for clarifying such a cascade diversity in various tissues.

Despite the complexity of its intracellular mechanisms, phenotypic outcomes indicated rather a simple translatability of Gpr83 for pain control. Both the reduction in Gpr83 level and the application of its ligand alleviated pain. The constitutive nature of Gpr83 and/or possible basal presence of an endogenous ligand may ordinarily contribute to the positive shift of the nociceptor activity, and the receptor removal may tune the activity balance downward. Extraneous additions of a ligand may drive a quick downregulation or desensitization of those tuning mechanisms. In this context, several pain control strategies can further be hypothesized, for instance, a concept of lowering Gpr83 expression by transcriptional regulation, a gene therapy approach for removing Gpr83, pharmacological modulations, etc. Among putative upstream factors for Gpr83 transcription, activating transcription factor 3 (Atf3), E1A binding protein P300 (Ep300), yin and yang 1 (Yy1), and zinc finger homeobox 2 (Zfhx2) have been confirmed in pain aggravation and gain translational attention [, 23, 33–35]. Future possible upstream modulators based on targeting these molecules may exert analgesic actions, at least in part, via controlling Gpr83 expression. Due to the ambivalent nature of Gpr83 observed in our experiments, it is also possible that inhibitors and agonists may both be effective at pain relief at a pharmacological aspect. Particularly, ligand-mediated results in our agonist assays are reminiscent of GPR downregulation strategies such as mimetics of gonadotropin-releasing hormone against some types of cancers and endometriosis [36, 37]. Collectively, a technology controlling expression and/or

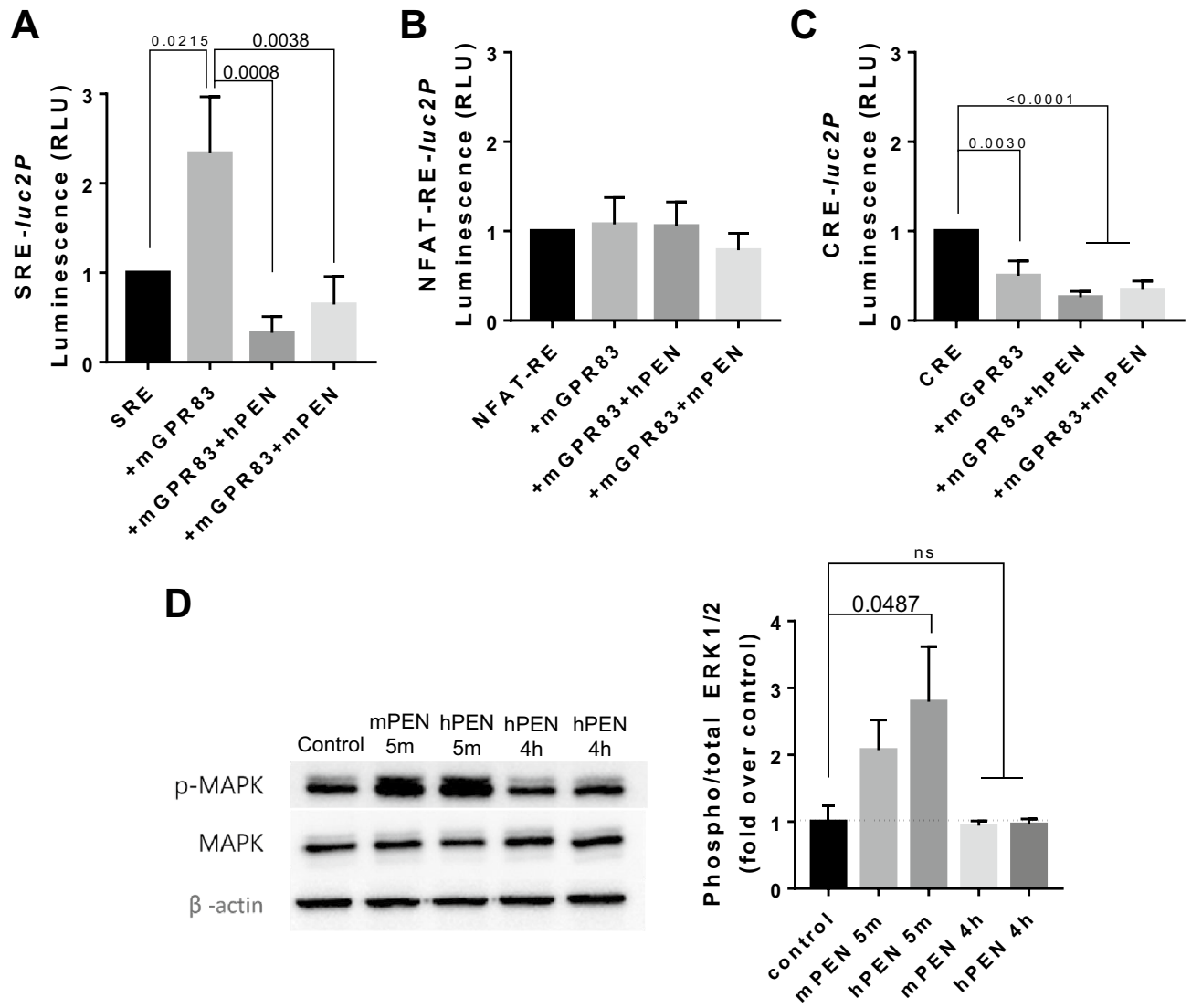

Fig. 7 PEN-induced signal transductions in luciferase assays. **A** Serum response element (SRE)-mediated luminescence was measured in mGpr83-transfected HEK cells with or without 4-h exposure to mouse PEN (mPEN) or human PEN (hPEN). Experiments were carried out in triplicate ($n=6$ batches). **B** Nuclear factor of activated T cell (NFAT)-mediated luminescence was measured in mGpr83-transfected HEK cells with or without 4-h exposure to mPEN or hPEN. Experiments were carried out in triplicate ($n=19$ batches). **C** cAMP response element (CRE)-mediated luminescence was measured in mGpr83-transfected HEK cells with or without 4-h exposure to mPEN or hPEN. Experiments were carried out in triplicate ($n=17$ batches). **D** Western blots (left) and their quantification (right) of extracellular signal-regulated kinase (ERK) with or without phosphorylation under PEN exposures. Data represent means ± S.E.M. ($n=4$, two-way ANOVA)

activity of Gpr83 can be an opportunity as a novel analgesic hypothesis in the future.

It remains to be conclusively determined how much the intrinsically constitutive activity of Gpr83 and the constant autocrine/paracrine actions, if any, of its endogenous ligands quantitatively contribute to its constantly tuning nature [10, 38, 39]. Other possibilities cannot completely be excluded, for instance, besides PEN there might be other endogenous ligands for Gpr83, and they may practically be more important if they are more readily and constantly secreted near nociceptors. Since Pcsk1n, the mother gene for producing PEN, and the cleavage enzymes generating its final form such as the subtilisin/kexin like proprotein convertases, furin, and carboxypeptidases, are all known to be expressed in DRG [40], PEN might be among the critical factors that activate Gpr83 in an autocrine manner. However, a related pain-relieving GPR, Gpr171 is also present in DRG neurons, and a similar enzymatic process may produce its specific ligand bigLEN from proSAAS, the protein that Pcsk1n encodes [4, 41]. Even more, Gpr171 was once proposed to

be able to interact with Gpr83 [26]. When the physiologically entangled GPR-ligand network is resolved, the translatability offered here will become more mechanistically clarified.

In conclusion, this study demonstrates that Gpr83 can modulate peripheral pain sensitivity via tuning nociceptor functions and thus suggests that controlling this GPR activity can be among promising concepts that help to alleviate pain.

Supplementary Information The online version contains supplementary material available at https://doi.org/10.1007/s13311-022-01327-3.

Required Author Forms Disclosure forms provided by the authors are available with the online version of this article.

Author Contribution Conceptualization, Y.K., C.K., S.W.H.; data curation, Y.K., C.K., H.L., J.Y.L., M.J.; funding acquisition, M.J., S.W.H.; investigation, Y.K.. C.K.; methodology, Y.K., H.L., C.K., J.Y.L., M.K., H.Z., J.C.; supervision, J.C., S.W.H.; writing—original draft, C.K., S.W.H.; writing—review and editing, Y.K., C.K., S.W.H.

Funding This work was supported by grants from the National Research Foundation of Korea (2017R1A2B2001817, 2019R1A4A1 029000, and 2022M3E5E8081190; S.W.H) and from Korea University Grant (K2208671; M.J.).

Data Availability All relevant data are available from the authors upon request.

Declarations

Competing Interests The authors declare no competing interests.

References

1. Woolf CJ. Capturing novel non-opioid pain targets. Biol Psychiatry. 2020;87:74–81.
2. Zheng H, Lim JY, Kim Y, Jung ST, Hwang SW. The role of oxytocin, vasopressin, and their receptors at nociceptors in peripheral pain modulation. Front Neuroendocrinol. 2021;63: 100942.
3. Berta T, Qadri Y, Tan PH, Ji RR. Targeting dorsal root ganglia and primary sensory neurons for the treatment of chronic pain. Expert Opin Ther Targets. 2017;21:695–703.
4. Cho PS, Lee HK, Choi YI, Choi SI, Lim JY, Kim M, Kim H, Jung SJ, Hwang SW. Gpr171 activation modulates nociceptor functions, alleviating pathologic pain. Biomed. 2021 Mar 5;9(3):256.
5. Zheng H, Lim JY, Seong JY, Hwang SW. The role of corticotropin-releasing hormone at peripheral nociceptors: implications for pain modulation. Biomed. 2020 Dec 17;8(12):623.
6. Jang Y, Kim M, Hwang SW. Molecular mechanisms underlying the actions of arachidonic acid-derived prostaglandins on peripheral nociception. J Neuroinflammation. 2020;17:30.
7. Ribeiro JML, Filizola M. Insights from molecular dynamics simulations of a number of G-protein coupled receptor targets for the treatment of pain and opioid use disorders. Front Mol Neurosci. 2019;12:207.
8. Coussens NP, Sittampalam GS, Jonson SG, Hall MD, Gorby HE, Tamiz AP, McManus OB, Felder CC, Rasmussen K. The opioid crisis and the future of addiction and pain therapeutics. J Pharmacol Exp Ther. 2019;371:396–408.
9. de Moerlooze L, Williamson J, Liners F, Perret J, Parmentier M. Cloning and chromosomal mapping of the mouse and human genes encoding the orphan glucocorticoid-induced receptor (GPR83). Cytogenet Cell Genet. 2000;90:146–50.
10. Gomes I, Bobeck EN, Margolis EB, Gupta A, Sierra S, Fakira AK, Fujita W, Müller TD, Müller A, Tschöp MH, Kleinau G. Identification of GPR83 as the receptor for the neuroendocrine peptide PEN. Sci Signal. 2016 Apr 26;9(425):ra43-.
11. Harrigan MT, Campbell NF, Bourgeois S. Identification of a gene induced by glucocorticoids in murine T-cells: a potential G protein-coupled receptor. Mol Endocrinol. 1991;5:1331–8.
12. Parker R, Liu M, Eyre HJ, Copeland NG, Gilbert DJ, Crawford J, Sutherland GR, Jenkins NA, Herzog H. Y-receptor-like genes GPR72 and GPR73: molecular cloning, genomic organisation and assignment to human chromosome 11q21.1 and 2p14 and mouse chromosome 9 and 6. Biochim Biophys Acta. 2000;1491:369–75.
13. Wang D, Herman JP, Pritchard LM, Spitzer RH, Ahlbrand RL, Kramer GL, Petty F, Sallee FR, Richtand NM. Cloning, expression, and regulation of a glucocorticoid-induced receptor in rat brain: effect of repetitive amphetamine. J Neurosci. 2001;21:9027–35.
14. Lachmann A, Torre D, Keenan AB, Jagodnik KM, Lee HJ, Wang L, Silverstein MC, Ma'Ayan, A. Massive mining of publicly available RNA-seq data from human and mouse. Nat Commun. 2018;9:1366.
15. Bang S, Yoo S, Yang TJ, Cho H, Hwang SW. Isopentenyl pyrophosphate is a novel antinociceptive substance that inhibits TRPV3 and TRPA1 ion channels. Pain. 2011;152:1156–64.
16. Choi G, Yang TJ, Yoo S, Choi SI, Lim JY, Cho PS, Hwang SW. TRPV4-mediated anti-nociceptive effect of suberanilohydroxamic acid on mechanical pain. Mol Neurobiol. 2019;56:444–53.
17. Bang S, Yoo S, Yang TJ, Cho H, Hwang SW. 17(R)-resolvin D1 specifically inhibits transient receptor potential ion channel vanilloid 3 leading to peripheral antinociception. Br J Pharmacol. 2012;165:683–92.
18. Moqrich A, Hwang SW, Earley TJ, Petrus MJ, Murray AN, Spencer KS, Andahazy M, Story GM, Patapoutian A. Impaired thermosensation in mice lacking TRPV3, a heat and camphor sensor in the skin. Science. 2005;307:1468–72.
19. Li Y, North RY, Rhines LD, Tatsui CE, Rao G, Edwards DD, Cassidy RM, Harrison DS, Johansson CA, Zhang H, Dougherty PM. DRG voltage-gated sodium channel 1.7 is upregulated in paclitaxel-induced neuropathy in rats and in humans with neuropathic pain. J Neurosci. 2018;38:1124–36.
20. Kinsey SG, Long JZ, O'Neal ST, Abdullah RA, Poklis JL, Boger DL, Cravatt BF, Lichtman AH. Blockade of endocannabinoid-degrading enzymes attenuates neuropathic pain. J Pharmacol Exp Ther. 2009;330:902–10.
21. Bang S, Yoo S, Yang TJ, Cho H, Hwang SW. Nociceptive and pro-inflammatory effects of dimethylallyl pyrophosphate via TRPV4 activation. Br J Pharmacol. 2012;166:1433–43.
22. Chatzigeorgiou M, Bang S, Hwang SW, Schafer WR. tmc-1 encodes a sodium-sensitive channel required for salt chemosensation in C. elegans. Nature. 2013;494:95–9.
23. Renthal W, Tochitsky I, Yang L, Cheng YC, Li E, Kawaguchi R, Geschwind DH, Woolf CJ. Transcriptional reprogramming of distinct peripheral sensory neuron subtypes after axonal injury. Neuron. 2020;108:128-144.e9.
24. Sharma N, Flaherty K, Lezgiyeva K, Wagner DE, Klein AM, Ginty DD. The emergence of transcriptional identity in somatosensory neurons. Nature. 2020;577:392–8.
25. Mack SM, Gomes I, Devi LA. Neuropeptide PEN and its receptor GPR83: distribution, signaling, and regulation. ACS Chem Neurosci. 2019;10:1884–91.
26. Müller A, Berkmann JC, Scheerer P, Biebermann H, Kleinau G. Insights into basal signaling regulation, oligomerization, and

structural organization of the human G-protein coupled receptor 83. PLoS ONE. 2016;11: e0168260.
27. Parobchak N, Rao S, Negron A, Schaefer J, Bhattacharya M, Radovick S, Babwah AV. Uterine Gpr83 mRNA is highly expressed during early pregnancy and GPR83 mediates the actions of PEN in endometrial and non-endometrial cells. F&S Science. 2020;1:67–77.
28. Choi SI, Hwang SW. Depolarizing effectors of bradykinin signaling in nociceptor excitation in pain perception. Biomol Ther (Seoul). 2018;26:255–67.
29. Toms C, Jessup H, Thompson C, Baban D, Davies K, Powrie F. Gpr83 expression is not required for the maintenance of intestinal immune homeostasis and regulation of T-cell-dependent colitis. Immunol. 2008;125:302–12.
30. Sah R, Parker SL, Sheriff S, Eaton K, Balasubramaniam A, Sallee FR. Interaction of NPY compounds with the rat glucocorticoid-induced receptor (GIR) reveals similarity to the NPY-Y2 receptor. Peptides. 2007;28:302–9.
31. Adams F, Grassie M, Shahid M, Hill DR, Henry B. Acute oral dexamethasone administration reduces levels of orphan GPCR glucocorticoid-induced receptor (GIR) mRNA in rodent brain: potential role in HPA-axis function. Brain Res Mol Brain Res. 2003;117:39–46.
32. Müller TD, Müller A, Yi CX, M Habegger K, Meyer CW, Gaylinn BD, Finan B, Heppner K, Trivedi C, Bielohuby M, Abplanalp W. The orphan receptor Gpr83 regulates systemic energy metabolism via ghrelin-dependent and ghrelin-independent mechanisms. Nat Commun. 2013 Jun 7;4(1):1-8.
33. Habib AM, Matsuyama A, Okorokov AL, Santana-Varela S, Bras JT, Aloisi AM, Emery EC, Bogdanov YD, Follenfant M, Gossage SJ, Gras M, Humphrey J, Kolesnikov A, le Cann K, Li S, Minett MS, Pereira V, Ponsolles C, Sikandar S, Torres JM, Yamaoka K, Zhao J, Komine Y, Yamamori T, Maniatis N, Panov KI, Houlden H, Ramirez JD, Bennett DLH, Marsili L, Bachiocco V, Wood JN, Cox JJ. A novel human pain insensitivity disorder caused by a point mutation in ZFHX2. Brain. 2018;141:365–76.
34. Hong S, Zheng G, Wiley JW. Epigenetic regulation of genes that modulate chronic stress-induced visceral pain in the peripheral nervous system. Gastroenterol. 2015;148:148-157.e7.
35. Sorge RE, Lacroix-Fralish ML, Tuttle AH, Khoutorsky A, Sotocinal SG, Austin JS, Melmed K, Labialle S, Schmidt JV, Wood JN, Naumova AK, Mogil JS. The Yin and Yang of pain: variability in formalin test nociception and morphine analgesia produced by the Yin Yang 1 transcription factor gene. Genes Brain Behav. 2013;12:405–13.
36. Kelly E, Bailey CP, Henderson G. Agonist-selective mechanisms of GPCR desensitization. Br J Pharmacol. 2008;153(Suppl 1):S379–88.
37. Rajagopal S, Shenoy SK. GPCR desensitization: acute and prolonged phases. Cell Signal. 2018;41:9–16.
38. Müller A, Kleinau G, Piechowski CL, Müller TD, Finan B, Pratzka J, Grüters A, Krude H, Tschöp M, Biebermann H. G-Protein Coupled Receptor 83 (GPR83) signaling determined by constitutive and zinc(II)-induced activity. PLoS ONE. 2013;8: e53347.
39. Tillmaand EG, Yang N, Kindt CAC, Romanova EV, Rubakhin SS, Sweedler. J. V. Peptidomics and secretomics of the mammalian peripheral sensory-motor system. J Am Soc Mass Spectrom. 2015;26:2051–61.
40. Zeisel A, Hochgerner H, Lönnerberg P, Johnsson A, Memic F, van der Zwan J, Häring M, Braun E, Borm LE, la Manno G, Codeluppi S, Furlan A, Lee K, Skene N, Harris KD, Hjerling-Leffler J, Arenas E, Ernfors P, Marklund U, Linnarsson S. Molecular architecture of the mouse nervous system. Cell. 2018;174:999-1014.e22.
41. Ram A, Edwards T, McCarty A, Afrose L, McDermott MV, Bobeck EN. GPR171 Agonist Reduces Chronic Neuropathic and Inflammatory Pain in Male, But Not Female Mice. Front Pain Res. 2021:62.